

# The Properties of the Magellanic Bridge Based on OGLE IV RR Lyrae Variables

R. Wagner-Kaiser,<sup>1\*</sup> Ata Sarajedini<sup>1†</sup>

<sup>1</sup>*University of Florida, Department of Astronomy, 211 Bryant Space Science Center, Gainesville, FL, 32611 USA*

## ABSTRACT

We examine the properties of the Magellanic Bridge connecting the Large and Small Magellanic Clouds using ab-type RR Lyrae variables from the extensive dataset of the Optical Gravitational Lensing Experiment (OGLE), Phase IV data release. The metallicities of the RR Lyraes are determined from the characteristics of their light curves, with an average abundance of  $[\text{Fe}/\text{H}] = -1.790 \pm 0.011$  (sem) in the Magellanic Bridge. From the individual reddenings of these stars, derived via their minimum light curve colors, we determined a median color excess of  $E(V-I) = 0.101 \pm 0.007$  (sem) (implying  $E(B-V) \approx 0.077$ ). The peak distance modulus of  $18.57 \pm 0.048$  (sem) places the Bridge stars at distances between the two systems. The metallicity and distance distributions probe the structure of the Magellanic system as a whole, revealing a smooth transition that connects the galaxies. An examination of the HI content does not find a clear correlation between HI emission strength and RR Lyrae spatial distribution, suggesting that the old stellar populations may trace the overlapping halo distributions of the two Magellanic Clouds.

**Key words:** stellar populations – RR Lyrae – LMC – dwarf galaxies.

## 1 INTRODUCTION

The Magellanic clouds are an important piece of the puzzle to help us better understand galaxy interactions, as well as the dynamical and star formation history of our own Galaxy. Not only do the gaseous features surrounding the Large and Small Magellanic Clouds (L/SMC) suggest past interactions between the two galaxies, but they also indicate the presence of a common HI envelope. However, there are still disagreements about the nature of these interactions, and the role of the Magellanic Bridge (MB) connecting the two galaxies. Some studies suggest that interactions between the LMC and SMC stem from multiple pericentric passages of the galaxies as they orbit our Galaxy, with the inter-galactic features resulting from tidal stripping and ram pressure (Růžička, Theis & Palouš 2009). Other work suggests that the Magellanic clouds have only begun interacting with each other and the Milky Way during two recent encounters, estimated to have occurred  $\sim 2$  Gyr and  $\sim 250$  Myr ago (Kallivayalil et al. 2013; Noël et al. 2015).

Proper motion and internal kinematics suggest that the MB likely resulted from a recent direct collision of the two galaxies (Kallivayalil et al. 2013; Besla et al. 2012; Diaz & Bekki 2012). Such an interaction is thought to have triggered

star formation in the MB, as pointed out by Grondin, Demers & Kunkel (1992); Mizuno et al. (2006); Skowron et al. (2014); Chen et al. (2014). However, based on their ages, the young stars could have either formed *in situ* in the MB, or formed in the SMC and been tidally stripped from it in the past  $\sim 200$  Myr (Noël et al. 2015).

Skowron et al. (2014) find that although the young stellar populations in the MB tend to be concentrated near the SMC, there is evidence for a continuity of a young population throughout the Bridge region, consistent with the HI densities. Intermediate age stellar populations have also been identified in the Bridge region, although they appear to occupy a distinctly different physical distribution than the pockets of star formation activity (Noël et al. 2013; Skowron et al. 2014; Noël et al. 2015). In particular, Skowron et al. (2014) find a non-uniform distribution of red giant and asymptotic giant branch stars across the region between the LMC and SMC.

Work by Borissova et al. (2004, 2006) suggests the existence of a stellar halo in the LMC based on velocity dispersion measurements of RR Lyrae variables, located as much as 2.5 degrees away from the center of the LMC. The large velocity dispersion of these stars ( $\sigma_{RV} = 50 \pm 2 \text{ km s}^{-1}$ ) indicates a homogeneous, old, and metal-poor halo. Other recent work has offered star counts as evidence that the LMC disk may extend to  $\sim 16$  kpc (Saha et al. 2010; Besla et al. 2016).

\*Email: rawagnerkaiser@astro.ufl.edu

†Email: ata@astro.ufl.edu

We now turn our attention to the tools we plan to employ in the present study. RR Lyrae variables provide valuable insights into the early formation epochs of galaxies (Sarajedini 2011; Smith 1995). Pulsating on the horizontal branch, these variable stars are quite old ( $\gtrsim 10$  Gyr), allowing us to look more closely at the ancient population of the Magellanic Bridge (Alcock et al. 2000; Soszyński et al. 2009). From the light curve shapes and characteristics of these stars, it is possible to determine not only distances, but also chemical properties and line-of-sight extinctions. The confluence of these many fundamental properties allows us a deep look into the history and evolution of their host galaxies.

The Optical Gravitational Lensing Experiment (OGLE, Udalski et al. 2012) has dramatically increased the number of RR Lyrae stars (and other types of variables) identified in the Magellanic system. Recent work has extended OGLE to even greater coverage of the LMC and SMC in Phase IV of the survey and now catalogs over 45,000 confirmed RR Lyrae variables (Soszyński et al. 2016), now including fields in the MB. While many previous studies have examined the RR Lyrae populations from the OGLE survey (Pejcha & Stanek 2009; Kinman et al. 1991; Haschke, Grebel & Duffau 2011; Haschke et al. 2012; Haschke, Grebel & Duffau 2012; Wagner-Kaiser & Sarajedini 2013; Deb & Singh 2014; Inno et al. 2016, among others), the recent expansion of spatial coverage allows a more detailed look at the old populations of the MB.

Here, we present a study of the reddening, metallicity, distance, and spatial distribution of RR Lyrae ab-type stars in the Magellanic Bridge between the LMC and SMC galaxies. Section 2 describes the dataset of the OGLE database. An analysis of the metallicities, distances, and reddenings of the RR Lyrae stars is presented in Section 3. Section 4 examines the HI content in the MB compared to the distribution of reddening and RR Lyrae positions. We conclude in Section 5.

## 2 DATA

In 1992, OGLE began with Phase I, with additional coverage (Phases II and III) released in following years (Udalski et al. 2012, 2003; Soszyński et al. 2009). The most recent dataset, OGLE Phase IV, extended the temporal and spatial coverage using the 1.3 meter Warsaw telescope at Las Campanas Observatory between March 2010 and July 2015 (Soszyński et al. 2016). Almost 500 fields of size 35 by 35 arcmin cover  $\sim 650$  square degrees of the sky in Cousins I-band and Johnson V-band filters, with the majority of the observations in the I-band.

Full details of the reduction procedures, photometric calibrations, and astrometric transformations may be found in Udalski et al. (2008) and Udalski, Szymański & Szymański (2015). Specifically, difference imaging techniques were employed to detect probable variables with periods between 0.2 and 1 day. Fourier decomposition and template fitting to the I-band light curves were used to preselect candidates, and periods were determined with a Fourier analysis (Soszyński et al. 2016).

The sample of ab-type RR Lyrae variables consists of 26,167 putative LMC stars and 4,750 in the SMC. The sam-

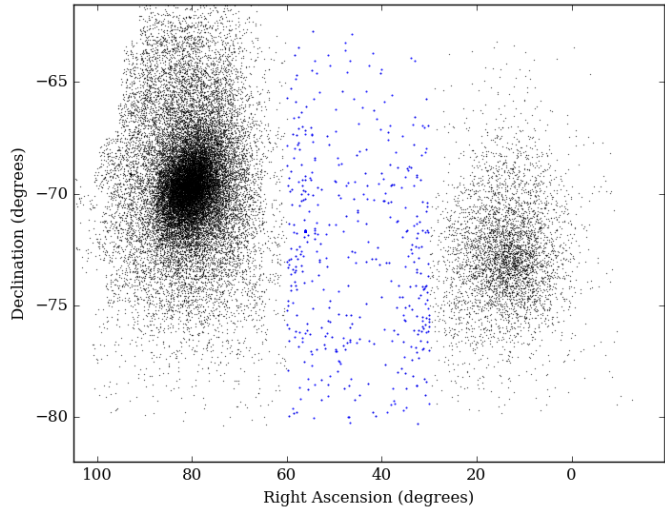


**Figure 1.** The RR Lyrae in OGLE classified as ab type are shown as black points, with the RR Lyrae falling into the Bridge region, indicated as blue points.

ples overlap in the area of the MB, as shown in Figure 1. In this figure, we have identified what we consider to be the MB variables as the blue points with the distribution of all identified OGLE RR Lyrae ab-type stars shown for comparison. We determine the Bridge region by eye to fall between the right ascensions of  $30^\circ$  and  $60^\circ$  (in the range of  $2^h$  and  $4^h$ ). There are 467 ab-type RR Lyrae stars in this region with well-determined magnitudes, I-band amplitudes, and periods; 452 of these stars also have well-determined Fourier parameters.

## 3 RESULTS

In Section 3.1, OGLE data are used to compare metallicities of ab-type RR Lyrae across the MB region. We derive extinctions for the RR Lyrae in Section 3.2, determined from the minimum light color of their light curves. The individual stellar reddenings are leveraged to examine the distribution of RR Lyrae distances in Section 3.3.

### 3.1 Metallicities

#### 3.1.1 RRab Stars

Metallicities for the RRab stars in our sample are found with the relationship from Alcock et al. (2000) shown in equation 1, which is on the Zinn & West (1984) abundance scale.  $P_{ab}$  represents the period of the ab-type variables and  $V_{amp}$  is the light curve amplitude in the V-band:

$$[Fe/H]_{ab} = -8.85[\log(P_{ab}) + 0.15V_{amp}] - 2.6. \quad (1)$$

However, to use equation 1, it is necessary to convert the I-band amplitudes from the OGLE IV catalog to V-band amplitudes. As in Wagner-Kaiser & Sarajedini (2013), we make use of equation 1 in Dorfi & Feuchtinger (1999):

$$V_{amp} = 0.075 + 1.497I_{amp}, \quad (2)$$

where  $V_{amp}$  and  $I_{amp}$  are the light curve amplitudes in the V- and I-band, respectively. Dorfi & Feuchtinger (1999) derive this empirical relation with a  $R^2$  correlation coefficient of 0.904.

While Alcock et al. (2000) estimate an error of  $\sim 0.31$  dex per star from Equation 1, the actual error may be less (Jeffery et al. 2011). Blazhko effects, which cause changes in amplitude over time, may affect some portion of RR Lyrae stars and incorporate errors up to 0.03 dex (Kunder, Chaboyer & Layden 2010). Additional errors of up to 0.014 dex may be introduced by the conversion of the I-band amplitude to the V-band value (Wagner-Kaiser & Sarajedini 2013). However, these two additional sources of error are negligible when compared to the overall error from Alcock et al. (2000).

For comparison, the metallicity is also derived from Fourier light curve decomposition parameters from the OGLE catalog via the I-band photometry. The methodology and derivation of the metallicity via Fourier parameters from Smolec (2005) has been recently updated by Skowron et al. (2016). We use this newer calibration of  $[Fe/H]$  to calculate the metallicity on the Jurcsik (1995) metallicity scale:

$$[Fe/H]_{J95,ab} = 2.132 - 5.394P_{ab} - 1.009\phi_{31} + 0.164\phi_{31}^2 \quad (3)$$

where  $P_{ab}$  is the period of the R Rab variables and  $\phi_{31}$  is a Fourier parameter. A phase change must be accounted for in  $\phi_{31}$ ; the OGLE Fourier decomposition uses a cosine series, while Skowron et al. (2016) uses a sine Fourier series.  $[Fe/H]$  is converted from Equation 3 from the Jurcsik (1995) metallicity scale to the Zinn & West (1984) scale (ZW):

$$[Fe/H]_{ZW,ab} = 1.028[Fe/H]_{J95,ab} - 0.242, \quad (4)$$

from Papadakis et al. (2000).

In Figure 2, the results are presented from our determination of  $[Fe/H]$  from Equations 1 through 4 for ab-type variables in the MB. In the left panel, the metallicity distribution from the Alcock et al. (2000) relation is presented (A00, blue), while the results from the Skowron et al. (2016) equation are shown in the right panel (S16, green). Gaussian profiles are fit to each of the metallicity distributions in Figure 2. The derived peak metallicities and errors representing the standard error of the mean are given in Table 1. The peak metallicity of the Bridge stars falls between the mean LMC and SMC metallicities.

The metallicities derived via the Fourier parameter method from Skowron et al. (2016) tend towards more metal-poor values, although the  $3\sigma$  errors from the two results marginally overlap. For comparison, metallicities from the literature are presented in Table 2. Also included in Figure 2 for comparison are vertical lines indicating the peaks of the LMC (dashed) and SMC (dotted) metallicity distributions from the OGLE dataset.

### 3.1.2 Metallicity Structure

From the abundances derived in Section 3.1, the metallicity of the RR Lyrae stars can be examined in the Bridge and across the Magellanic system. For each ab RR Lyrae variable in the Magellanic system, we calculate its projected radius:

**Table 1.** Peak Metallicity of Magellanic Bridge RR ab Lyrae

[Fe/H]	Method	Reference
$-1.744 \pm 0.016$	Equations 1 & 2	Alcock et al. (2000)
$-1.835 \pm 0.014$	Equations 3 & 4	Skowron et al. (2016)

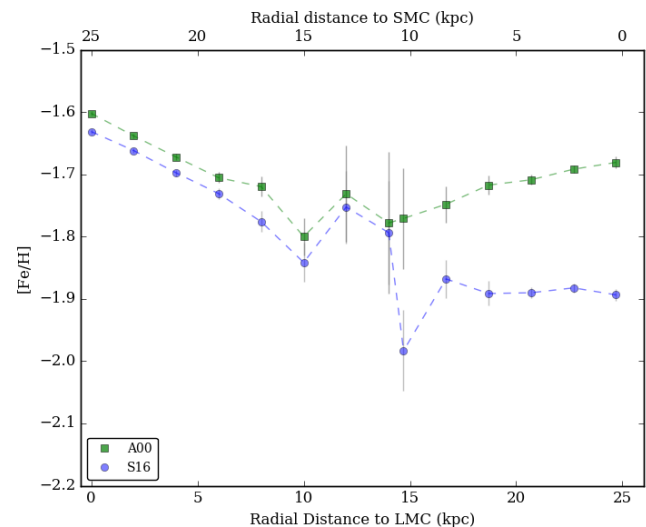


**Figure 3.** The metallicity binned every 2 kpc in distance from the center of the LMC on the lower abscissa and the center of the SMC from the upper abscissa. Metallicities are plotted for the Alcock et al. (2000) (green) and Skowron et al. (2016) (blue). The errorbars represent the standard error of the mean in each bin.

$$\cos \theta = [\sin(90 - \delta) * \sin(90 - \delta_{galx}) * \cos(\alpha - \alpha_{galx})] + [\cos(90 - \delta) * \cos(90 - \delta_{galx})], \quad (5)$$

from van der Marel & Cioni (2001), where  $\alpha_{galx}$  and  $\delta_{galx}$  are the right ascensions and declinations of the LMC center ( $5^h 23^m 34.5^s$ ,  $-69^\circ 45' 22''$ , van der Marel & Cioni 2001) and SMC center ( $0^h 55^m 7.2^s$ ,  $-72^\circ 47' 59''$ , Gonidakis et al. 2009). The variables  $\alpha$  and  $\delta$  are the right ascension and declination of the individual OGLE RR Lyrae stars. This is converted to a physical distance assuming an LMC distance modulus of 18.49 (de Grijs, Wicker & Bono 2014) and an SMC distance modulus of 18.96 (de Grijs & Bono 2015).

Figure 3 traces the metallicity changes across the Magellanic system. The stars are binned at intervals of 2 kpc and the mean and standard errors of the metallicities of the RR Lyrae are determined in each bin. After reaching an apparent minimum in the region of the Bridge, the overall metallicity becomes marginally more metal-rich near the SMC for the Alcock et al. (2000) metallicities and flattens out for the Skowron et al. (2016) derivation. The overall structure of the system is examined further in Sections 3.3 and 4.

### 3.2 Extinction

Guldenschuh et al. (2005) found the minimum light color of

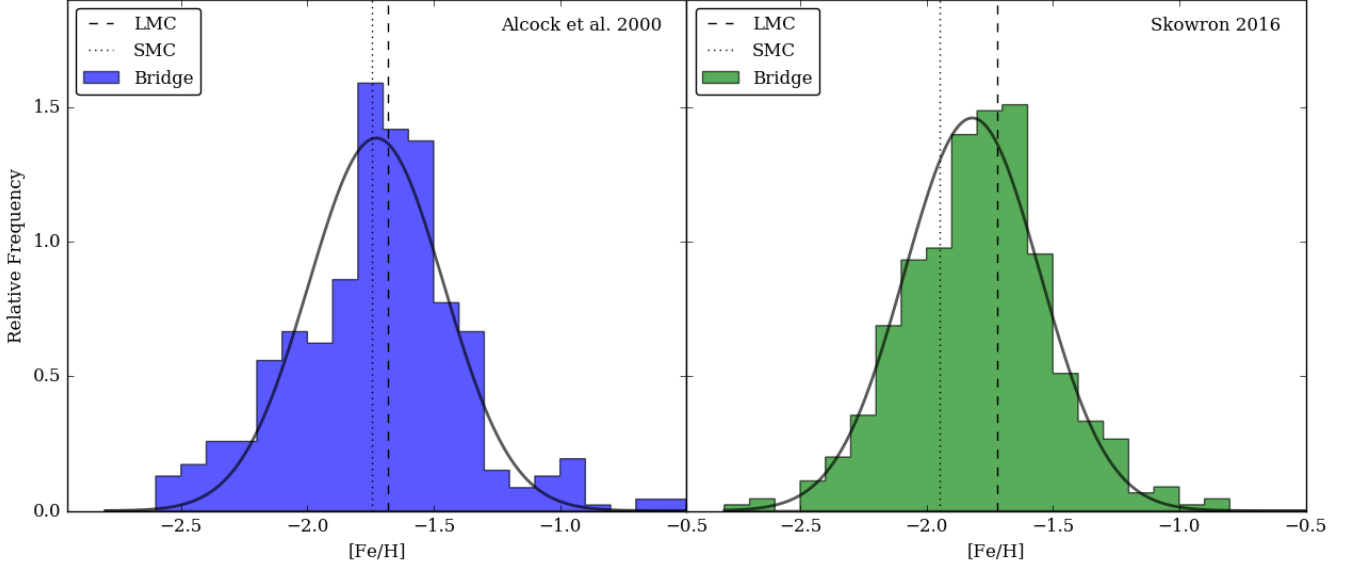


**Figure 2.** The distribution of RR Lyrae metallicities in the Magellanic Bridge determined from the Alcock et al. (2000) relation (A00, left) and those from Skowron et al. (2016) (S16, right). In each panel, Gaussians (black solid lines) are fit to each of the distributions. The peak LMC and SMC metallicities from these two approaches are indicated in each panel as dashed and dotted vertical lines, respectively. In both panels, the histograms are normalized to an area of 1.

**Table 2.** RR Lyrae Literature Metallicities

Galaxy	[Fe/H]	Method	Reference
LMC	$-1.70 \pm 0.25$	RRab, Alcock et al. (2000)	Wagner-Kaiser & Sarajedini (2013)
LMC	$-1.62 \pm 0.10$	RRab, Smolec (2005)	Wagner-Kaiser & Sarajedini (2013)
LMC	$-1.50 \pm 0.24$	RRab, Smolec (2005)	Haschke et al. (2012)
LMC	$-1.63 \pm 0.095$	Spectra	Borissova et al. (2006)
SMC	$-1.89 \pm 0.03$	RRab, Smolec (2005)	Kapakos & Hatzidimitriou (2012)
SMC	$-1.70 \pm 0.27$	RRab, Smolec (2005)	Haschke et al. (2012)

ab-type RR Lyrae variables, the color at the faintest point of the light curve, to be equal to  $(V - I)_o = 0.58 \pm 0.02$  regardless of their intrinsic properties. This relationship is used to determine individual reddenings for the RR ab stars in our LMC and SMC samples. From Guldenschuh et al. (2005), the  $E(V-I)$  reddening of an RR Lyrae ab star can be calculated by:

$$E(V - I) = (V - I)_{min} - 0.58. \quad (7)$$

If it is assumed that the ab-type RR Lyraes light curves are sinusoidal and symmetric, we can calculate the minimum light color for each star as:

$$(V - I)_{min} = [\langle V \rangle + \frac{A_V}{2}] - [\langle I \rangle + \frac{A_I}{2}], \quad (8)$$

where  $A_V$  and  $A_I$  are the V- and I-band amplitudes of the light curves.

However, because the shapes of ab-type RR Lyrae light curves are asymmetric and non-sinusoidal, this relation must be modified somewhat. From simulations, Wagner-Kaiser & Sarajedini (2013) determined a correction to be applied to

the minimum light color in Equation 8 using RRab light curve templates from Layden & Sarajedini (2000) as:

$$\Delta = (V - I)_{min}^{template} - [\langle V \rangle + \frac{A_V}{2}] - [\langle I \rangle + \frac{A_I}{2}]. \quad (9)$$

finding a mean value of  $\Delta$  for the 6 ab-type templates to be  $\langle \Delta \rangle = -0.061 \pm 0.017$ . We apply this correction to the minimum light colors derived from Equation 8 to account for the typically sawtooth, asymmetric ab-type light curves.

In Figure 4, the reddening distribution for the RRab stars in the MB is shown. A small percentage of the RR ab-type variables ( $\sim 5\%$ ) are found to have negative reddening values - a gratifyingly minimal amount. A Gaussian profile is fit to the reddening distribution, with a peak at  $E(V-I)$  of  $0.101 \pm 0.007$ , equivalent to  $E(B-V)$  of 0.077 assuming  $R_V = 3.1$ . The error in each individual reddening is  $\sigma = 0.026$  mag from the uncertainty in  $(V - I)_{o,min}$  and the non-sinusoidal correction. Table 3 shows a comparison of our reddening results for the LMC and SMC with those in the literature.

While the approach of Guldenschuh et al. (2005) rests on the somewhat contested presumption of an absolute minimum light color for RR Lyrae (supporting views: Kunder, Chaboyer & Layden 2010; Bhardwaj et al. 2014, opposing:

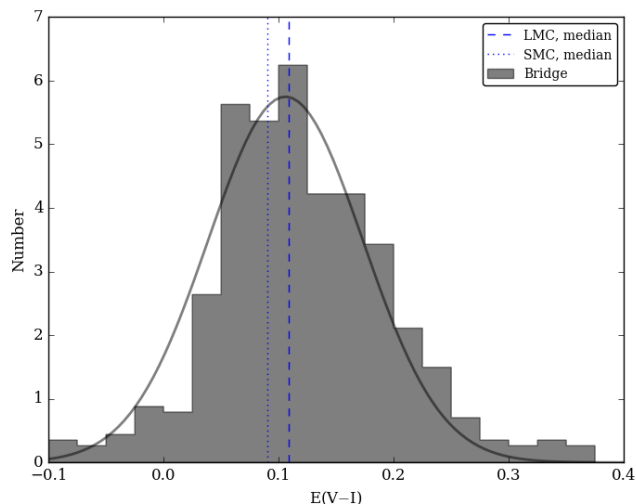


**Figure 4.** Histogram of reddening values for ab-type RR Lyraes in the Bridge, normalized to an area of 1. The solid line is the Gaussian fit to the central portion of the distribution. The peaks of the reddening distributions for the LMC and SMC are shown as dashed and dotted lines, respectively.

Collinge, Sumi & Fabrycky 2006; Layden, Anderson & Husband 2013), our estimates of the peak reddening from this approach fit well with other methods of reddening determination (see Table 3).

Upon examination of Figure 4, the reddening appears to be largely a continuous distribution. There is an overabundance beyond the Gaussian fit of the Bridge RR Lyrae for  $E(V-I) \gtrsim 0.15$ , which could be indicative of internal reddening affecting some Bridge stars. However, due to the uncertainties associated with reddening calculations and photometric uncertainties for individual stars ( $\approx 0.026$ ), it is difficult to disentangle. There is no clear bi-modality to separate the RR Lyrae affected by foreground reddening only and those affected by both foreground and internal reddening. We return to this in Section 4.

### 3.3 Distances

#### 3.3.1 RRab Stars

To determine individual distances to the RR ab variables, the relation from Chaboyer (1999) is used to relate the absolute magnitude to the metallicity of the stars:  $M_V = (0.23 \pm 0.04)([Fe/H] + 1.6) + (0.56 \pm 0.12)$ . We calculate the absolute magnitudes of the RR Lyrae with the OGLE mean V-band magnitudes, using the individual extinctions of each star (see Section 3.2).

The Alcock et al. (2000) and Skowron et al. (2016) derivations of the metallicity are both used to derive distances and the resulting distributions for the stars in the MB are compared in Figure 5. Gaussian profiles are fit to each distribution, with peaks for each provided in Table 4. The results from the two metallicity determinations are consistent exhibiting a difference of only 0.011 mag; the distances agree within the  $1-\sigma$  errors.

The peak distance of the RR Lyrae in the Bridge region is much more similar to the LMC than the SMC; this may suggest the Bridge RR Lyrae are dominated by stars more

**Table 4.** Peak Distance of Magellanic Bridge RR ab Lyrae

Distance Modulus	Method
$18.591 \pm 0.067$	Alcock et al. (2000)
$18.603 \pm 0.068$	Skowron et al. (2016)

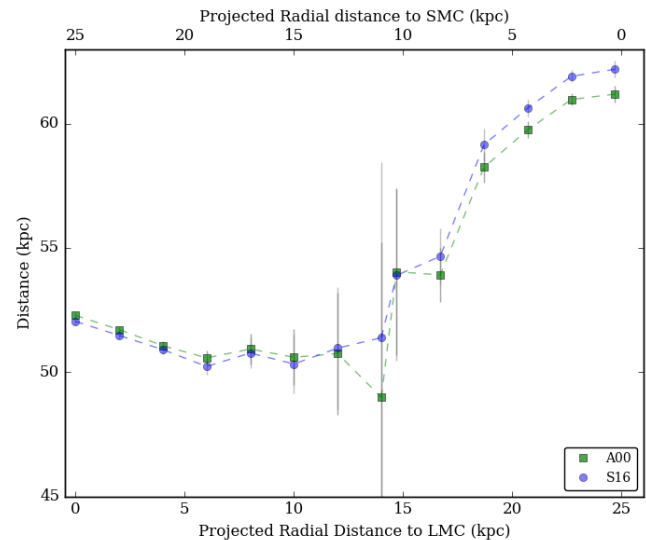


**Figure 6.** The mean distance of the RR ab variables along their projected radial distance in kpc from the center of the LMC-SMC system. The LMC is shown along the lower abscissa and the SMC is along the upper abscissa. We plot the distances derived from the Alcock et al. (2000) metallicity derivation in green and those from Skowron et al. (2016) in blue. For both derivations, there is a smooth transition of stellar distances that appears to connect the two galaxies in the Magellanic Bridge area. The errorbars represent the standard error of the mean in each bin.

likely to be associated to the LMC. We see less structure in the distance distribution derived via the Alcock et al. (2000) relation compared to Skowron et al. (2016). The latter has a possible secondary peak around the distance of the SMC at  $\mu \approx 18.9$ . The primary peak at the approximate distance of the LMC may again be indicative that the stars in the Bridge are largely from the LMC. However, a secondary peak is not clear in the Bridge distances derived via the Alcock et al. (2000) relation, though there tends to be an overabundance at higher distances.

#### 3.3.2 Structure of the Magellanic Bridge

The derived distances from Section 3.3 are used to examine the line-of-sight distribution of the ab-type RR Lyrae stars using their projected radial distances, binned every 2 kpc. As seen in Figure 6, the result shows a clear and smooth transition of stars between the two galaxies. This could be indicative of the overlapping halo distributions belonging to the LMC and SMC, as discussed further in Section 4.



**Table 3.** Literature Reddening

Galaxy	E(V-I)	Method	Reference
LMC	$0.12 \pm 0.05$	RRab OGLE III	Wagner-Kaiser & Sarajedini (2013)
LMC	$0.11 \pm 0.06$	RRab OGLE III	Haschke, Grebel & Duffau (2011)
LMC	$0.09 \pm 0.07$	Red Clump	Haschke, Grebel & Duffau (2011)
LMC	$0.11 \pm 0.06$	LMC Clusters	Wagner-Kaiser & Sarajedini (2013) (average from Johnson et al. (1999); Olsen et al. (1998); Brocato et al. (1996))
SMC	$0.07 \pm 0.06$	RRab OGLE III	Haschke, Grebel & Duffau (2011)
SMC	$0.04 \pm 0.06$	Red Clump	Haschke, Grebel & Duffau (2011)

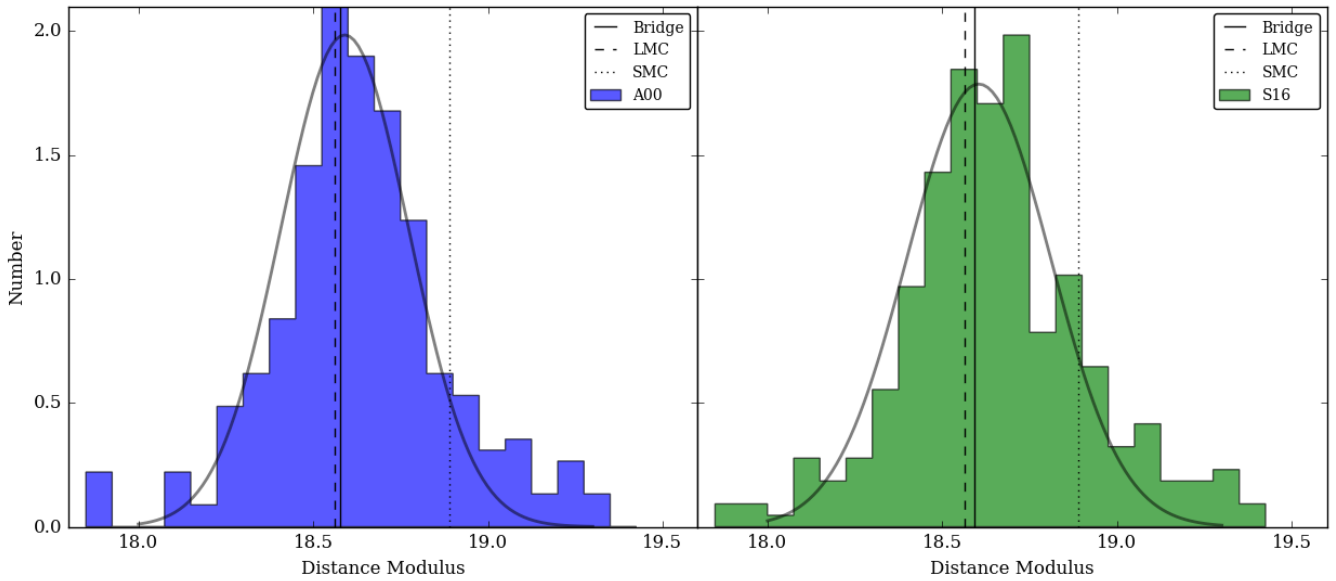


**Figure 5.** Distances derived from the Alcock et al. (2000) and Skowron et al. (2016) metallicity determinations are in blue and green, respectively, for the RR ab stars. The solid curve is the Gaussian distribution fitted to the distances of the Bridge RR Lyrae, with the peak indicated by the solid vertical line. The resulting Gaussian peaks are provided in Table 4 with the corresponding errors. In both panels, the histograms are normalized to an area of 1, and vertical lines indicating the median LMC (dashed) and SMC (dotted) distances from the OGLE RR Lyrae are plot for comparison.

## 4 THE MAGELLANIC BRIDGE

### 4.1 Extinction Analysis

As noted in Section 1, the Magellanic Clouds are a key component in understanding the early formation and evolution of the Milky Way system. The LMC and SMC are considered typical dwarf galaxies similar to the type that may have been accreted to form more massive galaxies, such as our own. Unlocking the history of the Magellanic Clouds thus helps shed light on the possible growth mechanisms of larger spiral galaxies as well as the local history of the Milky Way Galaxy and its satellites. By examining the Bridge between the LMC and SMC, we gain insight into the structure of the system and their history of interactions.

Studies have shown that the young and intermediate age stars in the MB have a clumpy, non-uniform distribution (Noël et al. 2013, 2015; Skowron et al. 2014). The asymmetric locations of these stellar populations suggest that either they formed in situ or were stripped from the LMC or the SMC during an interaction. However, the older RR Lyrae don't show any clear structure in their locations across that

region (e.g.: Figure 1). If the older populations, such as RR Lyrae, follow the trends of their younger counterparts, it would give credence to tidal stripping (as in-situ formation is not likely at such an early time in the Bridge). However, if the distribution of RR Lyrae is smooth across the Bridge, it may be indicative of an extended halo distribution of the SMC and LMC overlapping in the Bridge (Besla et al. 2016; Saha et al. 2010).

In Figure 7, we use HI observations of the LMC, SMC, and MB to examine RR Lyrae positions with respect to the HI integrated intensity (Putman et al. 2003). Visual inspection suggests there is not strong association between the physical distribution of the RR Lyrae and greater HI intensity.

To delve in further, the HI content of the region from Putman (2000) is compared to the extinction traced by the RR Lyrae (as per Section 3.2). The integrated HI intensity from Figure 7 is converted to a E(V-I) reddening through the following process. From Fukui et al. (2014), we can use Equation 10 to convert the integrated HI intensity,  $I_{HI}$ , to the column density,  $N_{HI}$ :

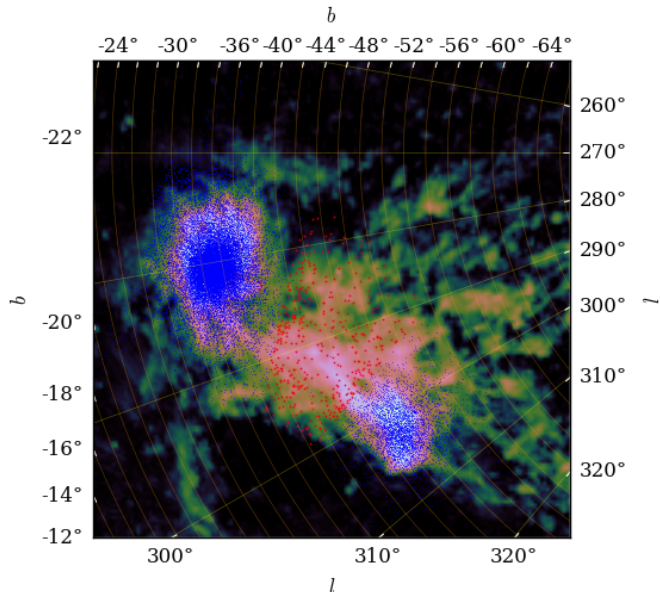


**Figure 7.** HI integrated intensity from Putman et al. (2003), overlaid with RR Lyrae locations from the OGLE survey indicated in blue. The RR Lyrae that fall into the Bridge region are indicated by the red points.

$$N_{HI}(cm^{-2}) = (1.823 \times 10^{18}) \times I_{HI}(Kkms^{-1}) \quad (10)$$

Following this, the  $E(B-V)$  is calculated from the HI column density using the relation from Bohlin, Savage & Drake (1978) and Diplas & Savage (1994):

$$N_{HI}(cm^{-2}) = (4.93 \pm 0.09) \times 10^{18} E(B-V) \quad (11)$$

Which is converted to  $E(V-I)$  with the relation  $1.32 \times E(B-V)$ , giving us an estimate of the amount of reddening caused by HI emission.

The reddening from the HI can now be compared to the RRL reddening across the Magellanic system, as seen in the top panel Figure 8. The HI content (blue squares) peaks near the centers of the LMC and SMC, and is lower but non-zero in the Bridge region. The reddening inferred from the RR Lyrae suggest greater extinction is present than accounted for by the HI content alone. However, HI does not explicitly trace dust content, although it is often taken as a proxy for the amount of extinction. CO observations of the broader region of the MB would give significant constraints on the dust content between the two galaxies. While presently CO observations are sparse in the Bridge region, focusing primarily on the disks of LMC and SMC (Wong et al. 2011), a study by Muller, Staveley-Smith & Zealey (2003) has found CO in the Bridge. New CO observations are likely to be expanded with ALMA; comparing the distribution of younger and older stellar populations to the existence of CO in the Bridge could provide direct evidence of star formation in the region.

We also compare the RR Lyrae reddening from Section 3.2 to the foreground reddening from Schlafly & Finkbeiner (2011) in the bottom panel of Figure 8. In general, the reddening derived from the RR Lyrae follows the general shape

of the foreground reddening; however, the high reddening near the centers of the LMC and SMC from the Schlafly & Finkbeiner (2011) foreground reddening is not reflected in the RR Lyrae values. Extinction experienced by the RR Lyrae stars above the foreground levels may be consistent with the existence of dust between the two galaxies. This may be consistent with the reddening histogram in Section 3.2, which displays an overabundance in the reddening distribution at higher  $E(V-I)$ .

It is worth checking how well the reddening implied by the RR Lyrae and that inferred for the foreground agree. To do this, we compare the Guldenschuh et al. (2005) method of using RR Lyrae colors to estimate an average reddening of the Galactic globular clusters to the reddening estimates of Schlafly & Finkbeiner (2011) (assuming  $E(B-V) = E(V-I)/1.32$ ). The comparisons are provided in Table 5. While there is scatter, the average offset between the two methods is only  $0.009 \pm 0.023$  (standard deviation)  $\pm 0.008$  (sem) mag, suggesting that the average RR Lyrae reddening is a reasonable tracer of extinction. This test lends credence to our observation that in the Magellanic system the estimation of foreground reddening from Schlafly & Finkbeiner (2011) underestimates the reddening traced by RR Lyrae in LMC. This indicates either the foreground extinction is consistently underestimating the reddening, or that extra dust is present in the MB, leading to additional reddening of RR Lyrae beyond the foreground reddening.

## 4.2 Discussion

If tidal interactions were key in the formation of the MB, we would expect to find an older population of stars in addition to the younger populations. Bagheri, Cioni & Napiwotzki (2013); Skowron et al. (2014); Noël et al. (2015) all present evidence of an older population of stars throughout the Bridge based on CMD analyses. The OGLE observations support this as well, with the presence of RR Lyrae variables in the Bridge confirming the residence of an old (at least 10 Gyr) stellar population. Figures 1 and 7 show that RR Lyrae appear to have a symmetric, non-clumpy distribution between the LMC and SMC, contrary to that of the younger populations.

Additionally, the analysis in Figures 7 and 8 do not present evidence that the RR Lyrae and HI intensity follow a coincident spatial distribution. Figure 7 does not reveal any clear association between areas of greater HI and RR Lyrae positions, supporting the idea that the old population is due in part to an overlapping of the two galactic halos. Figure 8 shows that the RR Lyrae population is affected by reddening beyond that traced by the foreground reddening.

Further, our analysis of the properties of the RR Lyrae in the bridge also suggest a gradual mixing of the LMC and SMC populations with distance between the galaxies. We find a clear, smoothly transitioning Magellanic Bridge between the LMC and SMC, as well as a transition from the relatively metal-rich LMC system to the slightly more metal-poor SMC system. These results provide evidence that the Bridge is made up of stars from both the LMC and SMC systems, similar to results from HIPASS data finding the Bridge HI content is likely contributed from both LMC and SMC material (Putman 2000). This is also suggested by Jacyszyn-Dobrzaniecka et al. (2016), whose work indicates that RR

**Table 5.** Comparison of Guldenschuh et al. (2005) and Schlafly & Finkbeiner (2011) Reddening of Galactic Globular Clusters

Cluster	$E(B-V)_{RRLyrae}$	$E(B-V)_{SF11}$	Difference	Reference
NGC 2808	0.163	0.1954	-0.0324	Kunder et al. (2013)
M 9	0.425	0.3746	0.0504	Arellano Ferro et al. (2016)
NGC 6981	0.053	0.0503	0.0027	Amigo et al. (2013)
M 22	0.291	0.2797	0.0113	Kunder et al. (2013)
NGC 3201	0.23	0.219	0.011	Arellano Ferro et al. (2016)
NGC 4590	0.05	0.0526	0.0026	Kains et al. (2015)
M 4	0.421	0.4285	-0.00771	Stetson et al. (2014)
M 5	0.065	0.0313	0.03362	Arellano Ferro et al. (2016)

Lyrae in the Magellanic Bridge region are from the overlapping halo distributions of the LMC and SMC through further exploration of the 3-D structure of the entire Magellanic system.

The sum of these results indicate that the older stellar populations in the MB were likely not affected by the same process as the younger populations, which are associated with HI and clumpy in their distribution across the MB. The older populations could be present in the MB due to either tidal stripping or the extended, overlapping stellar haloes of the LMC and SMC. The reddenings of the RR Lyrae indicate additional dust may be present in the bridge; dust could have been stripped with the old RR Lyrae from their host galaxies. The lack of correlation between HI and RR Lyrae positions implies this is not likely to be the case. Alternatively, the smooth transition in metallicity and distance could result from overlapping halo distributions of the LMC and SMC, which could explain a symmetric, smooth distribution of the old stellar populations.

Large-scale spectroscopic studies will be necessary to determine the LMC or SMC origins of individual stars; this would allow a determination of whether the old populations are overlapping haloes or stripped stars. Additionally, CO observations will be able to more accurately trace areas of high extinction and determine if there is any association with the distribution of stellar populations.

## 5 CONCLUSIONS

The new release of Phase IV from the OGLE survey is used to determine metallicities, reddenings, and distances of RR Lyrae stars in the LMC and SMC system. The analysis examines the metallicity gradients and extinction properties of both galaxies, including examining the properties of the Magellanic bridge and the kinematic properties of the Magellanic system. We present the following conclusions:

1. We derive distances, metallicities, and extinction for ab-type RR Lyrae in the Magellanic Bridge via established methodologies.
2. Examination of the distances between the LMC and SMC show a smooth transition in the distance and metallicities of the old stellar population between the LMC and SMC, connecting the two in a clearly defined Magellanic Bridge.
3. There is little coincidence between the clumpy HI intensity and smooth RR Lyrae positions. This indicates the older population of stars in the bridge may be better

explained by the overlap of the LMC and SMC haloes rather than tidally stripped stars.

## ACKNOWLEDGMENTS

We thank the anonymous referee whose comments and discussion were very helpful. Additionally, we would like to express our appreciation to Mary Putman for providing the HI images from the Parkes telescope.

## REFERENCES

- Alcock C. et al., 2000, *AJ*, 119, 2194  
Amigo P., Stetson P. B., Catelan M., Zoccali M., Smith H. A., 2013, *AJ*, 146, 130  
Arellano Ferro A., Ahumada J. A., Kains N., Luna A., 2016, *MNRAS*, 461, 1032  
Bagheri G., Cioni M.-R. L., Napiwotzki R., 2013, *A&A*, 551, A78  
Besla G., Kallivayalil N., Hernquist L., van der Marel R. P., Cox T. J., Kereš D., 2012, *MNRAS*, 421, 2109  
Besla G., Martínez-Delgado D., van der Marel R. P., Beletsky Y., Seibert M., Schlafly E. F., Grebel E. K., Neyer F., 2016, *ApJ*, 825, 20  
Bhardwaj A., Kanbur S. M., Singh H. P., Ngeow C.-C., 2014, *MNRAS*, 445, 2655  
Bohlin R. C., Savage B. D., Drake J. F., 1978, *ApJ*, 224, 132  
Borissova J., Minniti D., Rejkuba M., Alves D., 2006, *A&A*, 460, 459  
Borissova J., Minniti D., Rejkuba M., Alves D., Cook K. H., Freeman K. C., 2004, *A&A*, 423, 97  
Brocato E., Castellani V., Ferraro F. R., Piersimoni A. M., Testa V., 1996, *MNRAS*, 282, 614  
Chaboyer B., 1999, *Post-Hipparcos Cosmic Candles*, 237, 111  
Chen C.-H. R. et al., 2014, *ApJ*, 785, 162  
Collinge M. J., Sumi T., Fabrycky D., 2006, *ApJ*, 651, 197  
de Grijs R., Bono G., 2015, *AJ*, 149, 179  
de Grijs R., Wicker J. E., Bono G., 2014, *AJ*, 147, 122  
Deb S., Singh H. P., 2014, *MNRAS*, 438, 2440  
Diaz J. D., Bekki K., 2012, *ApJ*, 750, 36  
Diplas A., Savage B. D., 1994, *ApJ*, 427, 274  
Dorfi E. A., Feuchtinger M. U., 1999, *A&A*, 348, 815  
Fukui Y. et al., 2014, *ApJ*, 796, 59



- Gonidakis I., Livanou E., Kontizas E., Klein U., Kontizas M., Belcheva M., Tsalmantza P., Karampelas A., 2009, *A&A*, 496, 375
- Grondin L., Demers S., Kunkel W. E., 1992, *AJ*, 103, 1234
- Guldenschuh K. A. et al., 2005, *PASP*, 117, 721
- Haschke R., Grebel E. K., Duffau S., 2011, *AJ*, 141, 158
- Haschke R., Grebel E. K., Duffau S., 2012, *AJ*, 144, 106
- Haschke R., Grebel E. K., Duffau S., Jin S., 2012, *AJ*, 143, 48
- Inno L. et al., 2016, *ArXiv e-prints*
- Jacyszyn-Dobrzaniecka A. M. et al., 2016, *ArXiv e-prints*
- Jeffery E. J. et al., 2011, *AJ*, 141, 171
- Johnson J. A., Bolte M., Stetson P. B., Hesser J. E., Somerville R. S., 1999, *ApJ*, 527, 199
- Jurcsik J., 1995, *Acta Astron.*, 45, 653
- Kains N. et al., 2015, *A&A*, 578, A128
- Kallivayalil N., van der Marel R. P., Besla G., Anderson J., Alcock C., 2013, *ApJ*, 764, 161
- Kapakos E., Hatzidimitriou D., 2012, *MNRAS*, 426, 2063
- Kinman T. D., Stryker L. L., Hesser J. E., Graham J. A., Walker A. R., Hazen M. L., Nemec J. M., 1991, *PASP*, 103, 1279
- Kunder A., Chaboyer B., Layden A., 2010, *AJ*, 139, 415
- Kunder A. et al., 2013, *AJ*, 146, 119
- Layden A., Anderson T., Husband P., 2013, *ArXiv e-prints*
- Layden A. C., Sarajedini A., 2000, *AJ*, 119, 1760
- Mizuno N., Muller E., Maeda H., Kawamura A., Minamidani T., Onishi T., Mizuno A., Fukui Y., 2006, *ApJL*, 643, L107
- Muller E., Staveley-Smith L., Zealey W. J., 2003, *MNRAS*, 338, 609
- Noël N. E. D., Conn B. C., Carrera R., Read J. I., Rix H.-W., Dolphin A., 2013, *ApJ*, 768, 109
- Noël N. E. D., Conn B. C., Read J. I., Carrera R., Dolphin A., Rix H.-W., 2015, *MNRAS*, 452, 4222
- Olsen K. A. G., Hodge P. W., Mateo M., Olszewski E. W., Schommer R. A., Suntzeff N. B., Walker A. R., 1998, *MNRAS*, 300, 665
- Papadakis I., Hatzidimitriou D., Croke B. F. W., Papamastorakis I., 2000, *AJ*, 119, 851
- Pejcha O., Stanek K. Z., 2009, *ApJ*, 704, 1730
- Putman M. E., 2000, *PASA*, 17, 1
- Putman M. E., Staveley-Smith L., Freeman K. C., Gibson B. K., Barnes D. G., 2003, *ApJ*, 586, 170
- Růžička A., Theis C., Palouš J., 2009, *ApJ*, 691, 1807
- Saha A. et al., 2010, *AJ*, 140, 1719
- Sarajedini A., 2011, in *RR Lyrae Stars, Metal-Poor Stars, and the Galaxy*, McWilliam A., ed., Vol. 5, p. 181
- Schlaflly E. F., Finkbeiner D. P., 2011, *ApJ*, 737, 103
- Skowron D. M. et al., 2014, *ApJ*, 795, 108
- Skowron D. M. et al., 2016, *ArXiv e-prints*
- Smith H. A., 1995, *Cambridge Astrophysics Series*, 27
- Smolec R., 2005, *Acta Astron.*, 55, 59
- Soszyński I. et al., 2009, *Acta Astron.*, 59, 1
- Soszyński I. et al., 2016, *ArXiv e-prints*
- Stetson P. B. et al., 2014, *PASP*, 126, 521
- Udalski A. et al., 2012, *Acta Astron.*, 62, 133
- Udalski A., Pietrzynski G., Szymanski M., Kubiak M., Zebrun K., Soszynski I., Szewczyk O., Wyrzykowski L., 2003, *Acta Astron.*, 53, 133
- Udalski A., Szymanski M. K., Soszynski I., Poleski R., 2008, *Acta Astron.*, 58, 69
- Udalski A., Szymański M. K., Szymański G., 2015, *Acta Astron.*, 65, 1
- van der Marel R. P., Cioni M.-R. L., 2001, *AJ*, 122, 1807
- Wagner-Kaiser R., Sarajedini A., 2013, *MNRAS*, 431, 1565
- Wong T. et al., 2011, *ApJS*, 197, 16
- Zinn R., West M. J., 1984, *ApJS*, 55, 45

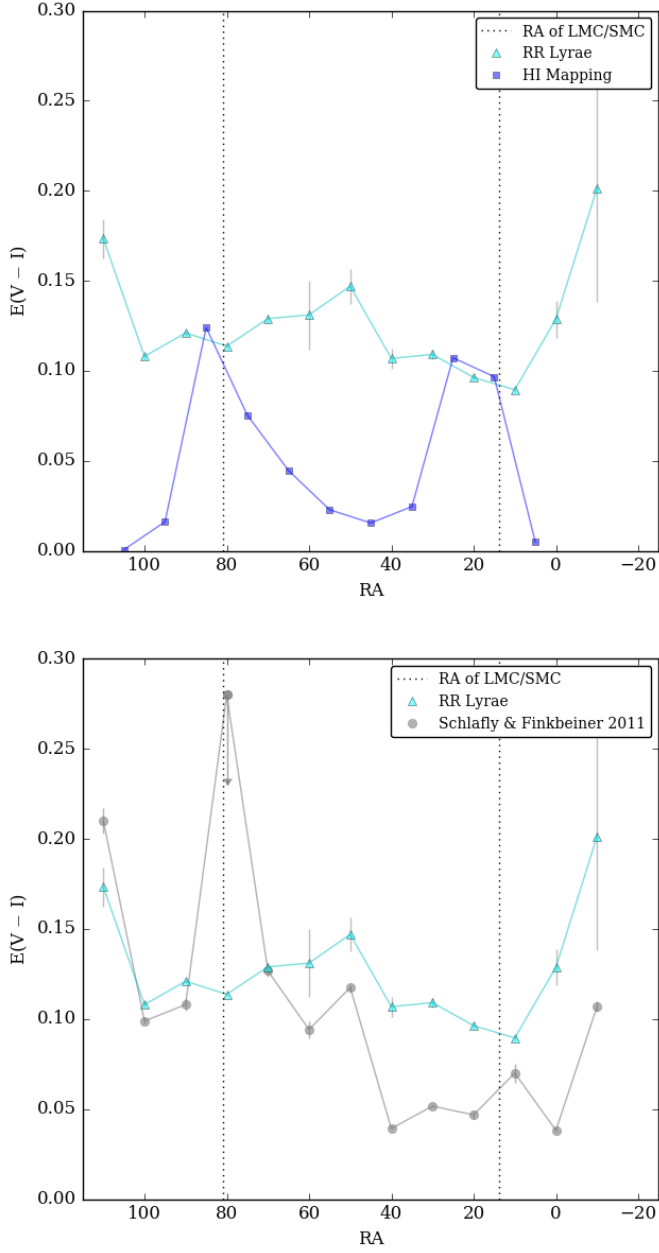


**Figure 8.** Distribution of median  $E(V-I)$  reddening values across the Magellanic system; we choose right ascension for the x-axis to clearly delineate the overall spatial behavior of the system. In the top panel, blue squares are binned  $E(V-I)$  values for the HI data from Figure 7, converted via Equations 10 and 11. Median binned reddenings derived via RR Lyrae from Section 3.2 are shown in cyan. In the bottom panel, the Schlafly & Finkbeiner (2011) foreground reddening from the COBE and DIRBE dust maps are shown as gray points and the RR Lyrae are again shown in cyan. In both panels, vertical lines indicate the centers of the LMC (left) and SMC (right). The errorbars represent the standard error of the mean in each bin.